Supplement of Atmos. Chem. Phys., 14, 8905–8915, 2014
http://www.atmos-chem-phys.net/14/8905/2014/
doi:10.5194/acp-14-8905-2014-supplement

Atmospheric Chemistry and Physics Open Access

Supplement of

Air–sea exchange and gas–particle partitioning of polycyclic aromatic hydrocarbons in the Mediterranean

M. D. Mulder et al.

Correspondence to: G. Lammel (lammel@recetox.muni.cz)

Supplementary Material

Polycyclic aromatic hydrocarbons in atmospheric aerosols and air-sea exchange in the Mediterranean

Marie D. Mulder[a], Angelika Heil[b], Petr Kukučka[a], Jana Klánová[a], Jan Kuta[a], Roman Prokeš[a], Francesca Sprovieri[c], Gerhard Lammel[a,d]

[a] Masaryk University, Research Centre for Toxic Compounds in the Environment, Brno, Czech Republic
[b] Helmholtz Research Centre Jülich, Institute for Energy & Climate Research, Jülich, Germany
[c] CNR, Institute for Atmospheric Pollution Research, Rende, Italy

[d] Max Planck Institute for Chemistry, Mainz, Germany

12 pages, 3 tables and 5 figures

S1. Methodology
S1.1 Sampling

Table S1. Sampling times of high-volume air samples

Air sample	Start time (UTC)	Stop time (UTC)	Duration (h)
1	27.8.10 20:00	29.8.10 08:00	36
2	29.8.10 11:30	30.8.10 16:30	29
3	30.8.10 16:45	31.8.10 13:45	21
4	31.8.10 15:00	1.9.10 12:00	21
5	1.9.10 13:00	2.9.10 13:00	24
6	2.9.10 13:30	3.9.10 18:30	29
7	3.9.10 20:15	4.9.10 18:15	22
8	4.9.10 20:00	5.9.10 04:00	8
9	5.9.10 06:10	5.9.10 22:10	16
10	6.9.10 01:00	7.9.10 10:00	33
11	7.9.10 12:15	8.9.10 06:15	18
12	8.9.10 08:30	8.9.10 18:10	9.4
13	8.9.10 19:00	9.9.10 06:00	11
14	9.9.10 16:30	10.9.10 09:00	16.3
15	11.9.10 20:00	12.9.10 06:00	10

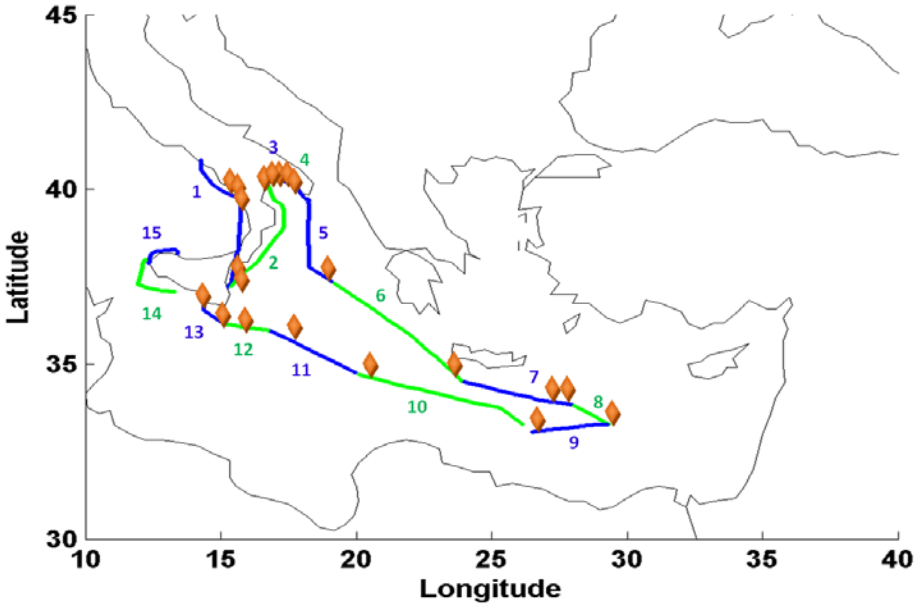

Figure S1. Spatial coverage of air (blue and green, numbers) and seawater samples (diamonds)

S1.2 Diffusive air-sea exchange flux calculation

A sensitivity analysis was done to explore the influence of the variabilities of air and seawater temperatures and wind speed (expressed as their standard deviations) during individual sample duration on the air-sea exchange flux (Table S2).

Table S2. Sensitivity, S_F, of the diffusive air-sea exchange flux, F_{aw}, calculated as $S_F = |\,[100\times (F_{aw} + \sigma_i) - F_{aw}]/F_{aw}\,|$, with the standard deviations, σ_i, of i = wind speed (WS) or air or seawater temperature (T_a, T_w). See main text for PAH acronyms.

	FLT	PYR	RET
WS	146	148	185
T_a	1.3	0.19	4.1
T_w	13	9.5	4.1

S1.3 Two-box fugacity model

A non-steady state 2-box model was applied to test the hypothesis that seasonal depositional input of RET into the surface waters during the fire season (summer) triggers reversal of diffusive air-sea exchange.

The model simulations for the period 2005-2010 were initialised by fire-related RET emissions into air for the East Mediterranean (28-45°N, 8-30°E). RET was in the region eventually also emitted to air from coal and crop residues combustion (Bi et al., 2008; Shen et al., 2012), and eventually emitted to seawater influenced by pulp or paper mill effluents (Leppänen and Oikari, 1999) or by diagenesis (Alexander et al., 1995) in the region. However, these sources of RET to air and seawater are neglected as expected to contribute insignificantly and to show less inter-annual variability. Moreover, advection of RET into the model domain e.g., from fires in the western Mediterranean is neglected for simplicity.

Temperature and wind speed data were taken from the Iraklion meteorological station (35°20'N / 25°11'E, 39 m above sea level), located close to the centre of the model domain. Wind speed data were extrapolated to 10 m above sea level assuming neutral conditions all the time (Stull, 1988). Input data are listed in Table S3. Only wind speeds of on-shore winds were considered representative, while periods (hourly data) of off-shore winds observed at Iraklion were rejected, leading to gaps in the time series of predicted F_{aw}. No experimental data for RET lifetime in seawater exist. Degradation rate in seawater is uncertain. It was derived from a model estimated halflife against hydrocarbon biodegradability in freshwater (56 days; BioHCwin; USEPA, 2009), which could be much longer for seawater. A factor of 10 is often applied to estimate lifetime in seawater from data in freshwater (EU, 1996).

Gaseous air and seawater concentrations and the air-sea exchange flux, F_{aw}, are output.

Two scenarios are considered, an 'Initially Estimated Parameter Set' (IEPS) representing mean values for environmental parameters, and an 'Upper Estimate Parameter Set' (UEPS) which represents realistic environmental conditions favouring seawater pollution (Table S3). UEPS considers lower estimates for the atmospheric and seawater mixing layers, the degradation rate in seawater (k_{OC}) and the export (settling) velocity in seawater (v_{exp}) and an upper estimate of the of fire-related $PM_{2.5}$ emission flux.

Table S3. Input parameters for the 2-box model, initially estimated parameter set (IEPS). For the upper estimate parameter set (UEPS) FRPM25 was replaced by FRPM25×5, KOC by KOC/100, VEXP by VEXP/10, HMIX by HMIX/2, and HMIXM by HMIXM/2.

	Parameter	Unit	Value adopted or mean (min-max)	Reference
COH	OH concentration in air	molec cm^{-3}	$(0.5\text{-}2.2)\times10^{6}$ during day-time, 0 during nighttime	climatological data (Spivakovsky et al., 2000) temporally interpolated
DOC	Dissolved organic carbon	µM	61.5	Pujo-Pay et al., 2011
FRPM25	fire-related $PM_{2.5}$ emission flux	mg m^{-2} h^{-1}	$3.02\ (0 - 496)\times10^{-7}$	Kaiser et al., 2012
FACEMPM25	Emission factor for $PM_{2.5}$	mg (kg fuel burnt)$^{-1}$	207	Schmidl et al., 2008, Andreae 1991
HENRY	Henry coefficient of RET	Pa m^{-3} mol^{-1}	2.3	USEPA, 2009
HMIX	Atmospheric mixing height	M	1000	Estimate
HMIXM	Mixing depth in ocean	M	40	d'Ortenzio et al., 2005
KDOC	Dissolved organic carbon/water partition coefficient	L g^{-1}	158.49	Karickhoff, 1981
KOC	1st order degradation rate coefficient in seawater	s^{-1}	1.0×10^{-7} (4×10^{-8} - 4×10^{-7})	USEPA, 2009, T dependence: EU, 1996
KOH	Gas-phase reaction rate coefficient with OH of RET	cm^3 $molec^{-1}$ s^{-1}	4.2×10^{-11}	Lammel et al., 2010a
KOW	Octanol/water partitioning coefficient of RET		2.24×10^{6}	USEPA, 2009
KOHEOR	Factor E/R in van 't Hoff equation for OH reaction of RET	K	-20.33	Calvert et al., 2002
KPOC	Particulate organic carbon/water partitioning coefficient	L g^{-1}	2240	assumed to be given by K_{ow}; Rowe et al., 2009

KS	Setschenow constant of RET	L mol^{-1}	0.38	Jonker and Muijs, 2010
POC	Concentration of particulate organic carbon in surface seawater	µM	3.08	Pujo-Pay et al., 2011
T_a	Air temperature	K	292.1 (275.2 - 311.2)	WMO, 2013
T_w	Surface seawater temperature	K	292.1 (27482 - 311.6)	estimated from T_a: $T_w = T_a + 0.4$ K during day-time, $T_w = T_a - 0.4$ K during nighttime
THETA	Particulate mass fraction of RET in air		0.05 (0.02 - 0.14)	Lammel et al., 2010a, T dependence: Lammel et al., 2010b
VEXP	Export (settling) velocity of particle-sorbed molecule in seawater	m s^{-1}	8×10^{-6}	Schwarzenbach et al., 2003
VDEPP	Deposition velocity of particle-sorbed molecule in air	m s^{-1}	6.5×10^{-5}	Franklin et al., 2000
WS	Wind speed	m s^{-1}	6.1 (0.6-30.7)	WMO, 2013

S2. Results

S2.1 Gas-particle partitioning

a.

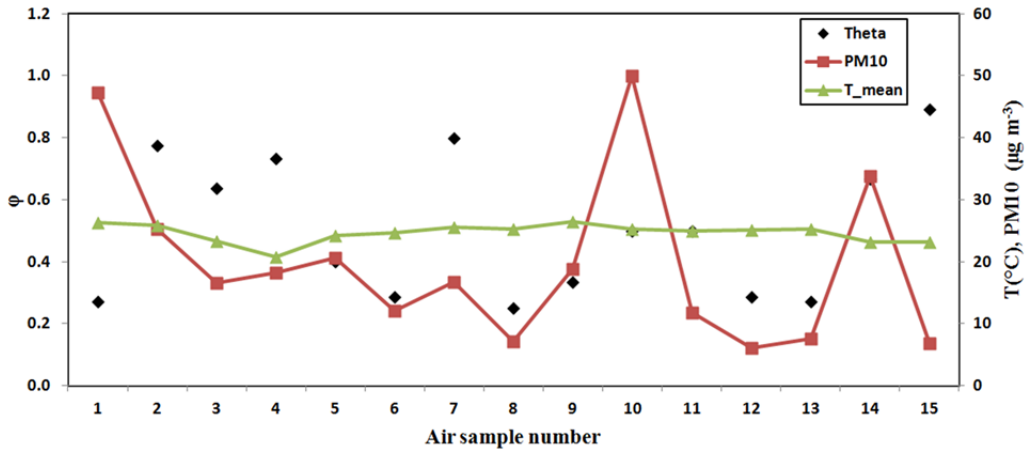

b.

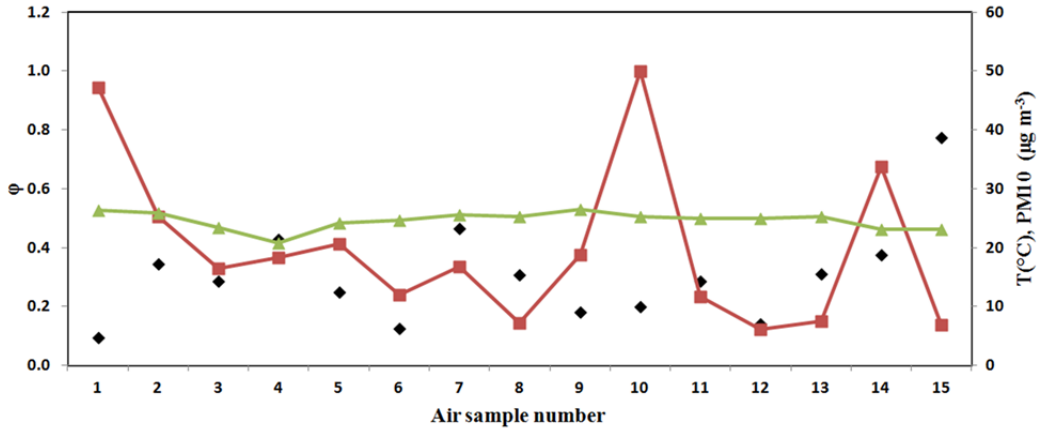

c.

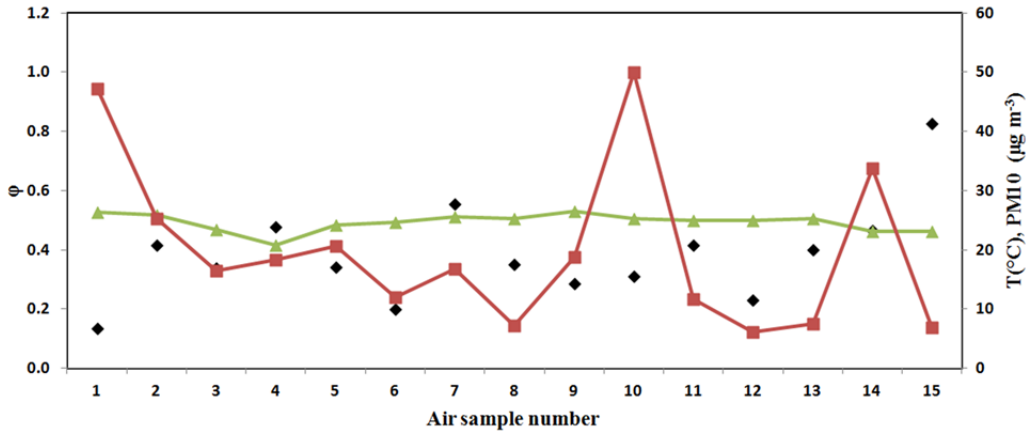

d.

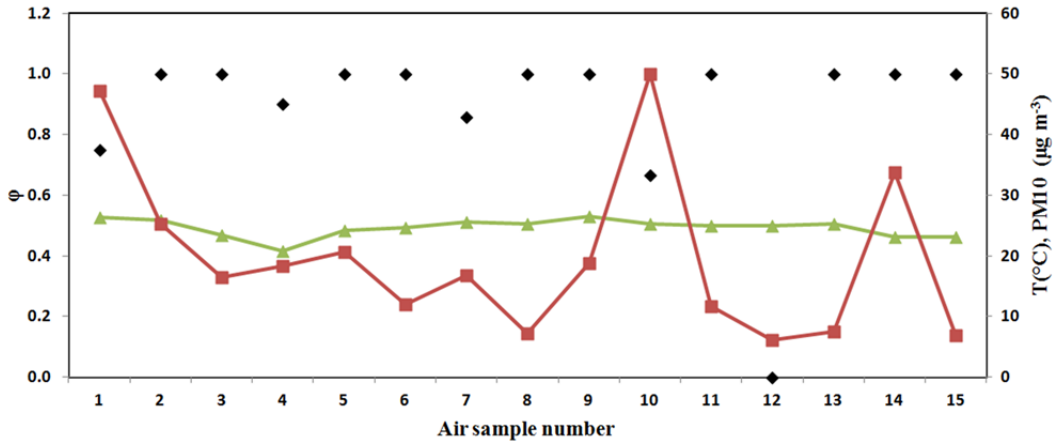

Fig. S2. Time series of particulate mass fraction (Theta), air temperature T(°C) and PM_{10} concentration (ng m^{-3}) for (a) BAA, (b) TRI, (c) CHR and (d) BBF.

The concentrations found in the stage corresponding to smallest particles, <0.25 µm, are shown in Table S4. Concentrations in size fractions corresponding to larger particles were <LOQ, except for CPP in one sample, resulting in 0.002 (<0.001-0.006) ng m^{-3} CPP in the size fraction corresponding to 0.5-1.0 µm. We refrain from reporting results of 2-3 ring PAHs in impactor samples, as due to vapour pressure very small particulate mass fractions are expected and LOQ were partly high. While all other PAHs particulate phase concentrations based on low-volume impactor measurement (Table S4) are consistent with those based on high-volume sampling (Table 1a), this is not the case for RET (higher concentration in particulate phase size fraction corresponding to <0.25 µm than as total atmospheric concentration from high-volume sampling). This is unexplained and may be related to loss of RET from the QFF.

Table S4. Concentrations of 4-6 ring PAHs found in particulate phase size fraction corresponding to <0.25 μm aerodynamic diameter (AD) (ng m^{-3}) as time-weighted mean (min-max). n_{LOQ} = number of samples > LOQ (out of 3). PAHs with concentrations <LOQ in all size fractions not listed. LOQ = 0.001 ng m^{-3} except for FLT (0.011) and PYR (0.020).

	n_{LOQ}	mean (min-max)
FLT	3	0.046 (0.035–0.054)
PYR	3	0.047 (0.040–0.051)
RET	3	0.048 (0.046–0.050)
CPP	1	0.007 (<0.001–0.022)
CHR	1	0.002 (<0.001–0.005)
BJF	1	0.002 (<0.001–0.007)
BEP	1	0.003 (<0.001–0.008)

S2.2 Air-sea exchange

S.2.2.1 FLT and PYR

FLT, PYR and dimethylphenanthrenes were near equilibrium or net volatilisational in coastal waters of the southeastern Mediterranean and FLT in the Black Sea, and also FLT (FR = f_a/f_w = 0.1) and PYR (FR = 0.3) in two pairs of samples collected in May 2007 in the open southeastern Mediterranean Sea, in the same regions as our samples No. 8 and 10 (Castro-Jiménez et al., 2012). In this study (June-July 2006 and May 2007), for FLT and PYR mean deposition fluxes F_{aw} = -5.87 (-11.42 – -1.11) ng m^{-2} d^{-1} and F_{aw} = -7.29 (-12.18 – -2.46) ng m^{-2} d^{-1}, respectively, were derived in the ISS, while for the SEM for FLT and PYR mean volatilisation fluxes F_{aw} = 14.33 (4.54 – 41.04) ng m^{-2} d^{-1} and F_{aw} = 15.90 (-0.56 – +62.58) ng m^{-2} d^{-1}, respectively, were derived. In our study (August-September 2010), in the ISS (paired air and water samples No. 11-13) we obtain F_{aw} = 3.14 (-38.79 – +29.16) ng m^{-2} d^{-1} and F_{aw} = 60.95 (-14.21 – +195.0) ng m^{-2} d^{-1} for FLT and PYR, respectively, and for the SEM (paired air and water samples No. 7-10) F_{aw} = - 47.36 (-169.23 – +24.45) ng m^{-2} d^{-1} and F_{aw} = -53.64 (-243.67 – +62.74) ng m^{-2} d^{-1} for FLT and PYR, respectively. This

comparison shows opposite findings. However, spatial variability was very high during the 2010 cruise: In the ISS different signs of flux are indicated for the various sampling sites. In the SEM the mean fluxes derived from the paired air and water samples No. 7 and 9-10 (neglect of samples No. 8), F_{aw} = 7.48 (-2.62 - 24.45) and F_{aw} = 42.64 (17.73-62.74) for FLT and PYR, respectively, is close to the 2006-07 findings. C_a in sample No. 8 was very high, apparently because the air mass had passed over an industrial area in western Turkey (Izmir; see also Fig. S4a). This caused a correspondingly high deposition flux, similar to the mean annual fluxes derived for 2001-02 at Finokalia, Crete, with then lower C_w (i.e., F_{aw} = -240 ng m^{-2} d^{-1} and F_{aw} = -187 ng m^{-2} d^{-1} for FLT and PYR, respectively; Tsapakis et al., 2006). In conclusion, considering spatial and temporal variabilities and different seasons (spring vs. summer) no trend, in particular no reversal of air-sea exchange is indicated by these two data sets, 3 years apart.

S2.2.2 RET

Under UEPS (Fig. S3), for 6 out of 12 observed (i.e., fugacity ratio-derived) F_{aw} (all > 0) agreement within one order of magnitude is found (underpredicting), the wrong sign (F_{aw} < 0) is predicted for 2 such cases (31.8.2010 and 2.9.2010) and no prediction was possible for 4 such cases. Note that because of a high frequency of nocturnal off-shore winds at the coastal station from where wind speed data were adopted (land breeze at Iraklion, Crete), data gaps in the simulated time series of F_{aw} occur more often during night-time than during day time (visible in Fig. S3). Because of the diurnal variation of temperature and wind speed these data gaps are often corresponding with maxima rather than minima of predicted F_{aw}. Underprediction could be due to neglected emissions to air and seawater in the region other than fire related (no or little seasonality) or neglect of advection into the model region (similar seasonality as captured emissions). Therefore, also the amplitude of the high frequency (daily) fluctuations could be underestimated. On the other hand, F_{aw} derived from observed concentrations C_a and C_w is uncertain, too. The biggest contribution is expected to be caused by sampling air and water not simultaneously (but combining short seawater sampling intervals with 10-20 h air sampling periods, often starting or ending when seawater samples were collected).

A sensitivity analysis (section S1.2) was performed to quantify the uncertainty of the calculated flux, F_{aw}, accounting for the variabilities of wind speed, air and seawater temperatures during sampling periods (Table S2). F_{aw} is found most sensitive to wind speed, changes on average for all the samples about 160% when adding or subtracting one SD of wind speed (hourly data) from the mean. The flux is much less sensitive to variation of the air and seawater temperatures, leading to changes of approximately 2 and 9%, respectively, when adding or subtracting one SD from the mean. While the sensitivity of F_{aw} to wind speed would be even higher when based on higher time-resolved data, hourly data appear appropriate considering mixing times of surface waters. This sensitivity to input uncertainties may explain part of the underestimate, but not up to one order of magnitude.

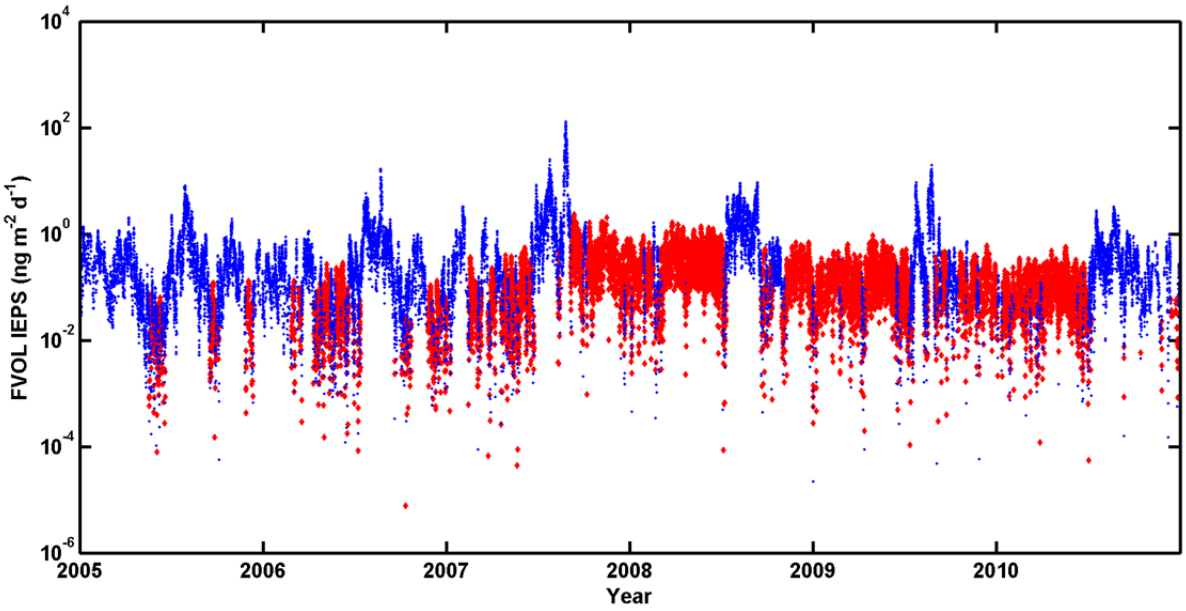

Fig. S3. Model predicted diffusive air-sea exchange flux, F_{aw}, of RET (ng m^{-2} d^{-1}; downward in blue and upward in red) using the initially estimated parameter set (IEPS) for the Eastern Mediterranean (28-45ig°N/8-30°E) 1.1.2005-31.12.2010, hourly means. Data filtered against off-shore winds (see main text). (Same as Fig. 3, but IEPS)

S2.3 Long-range transport

a)

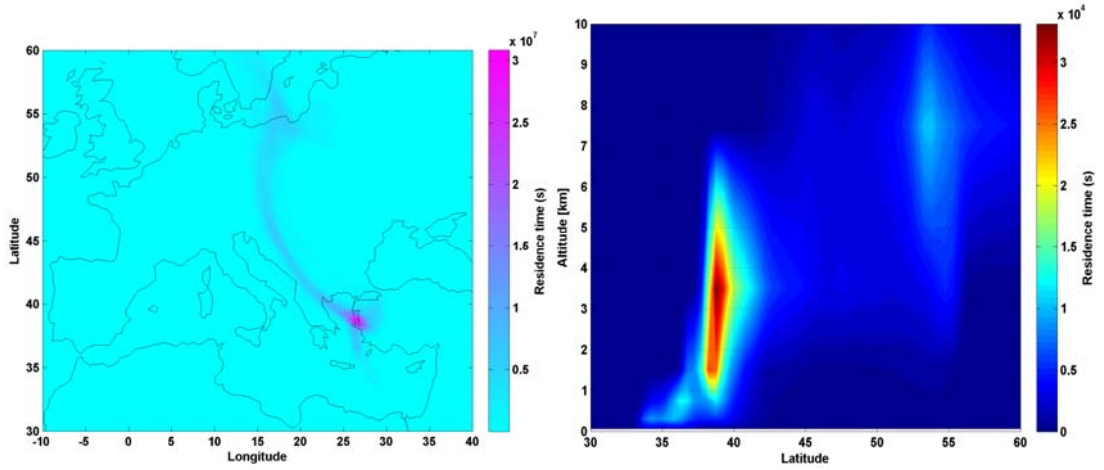

b)

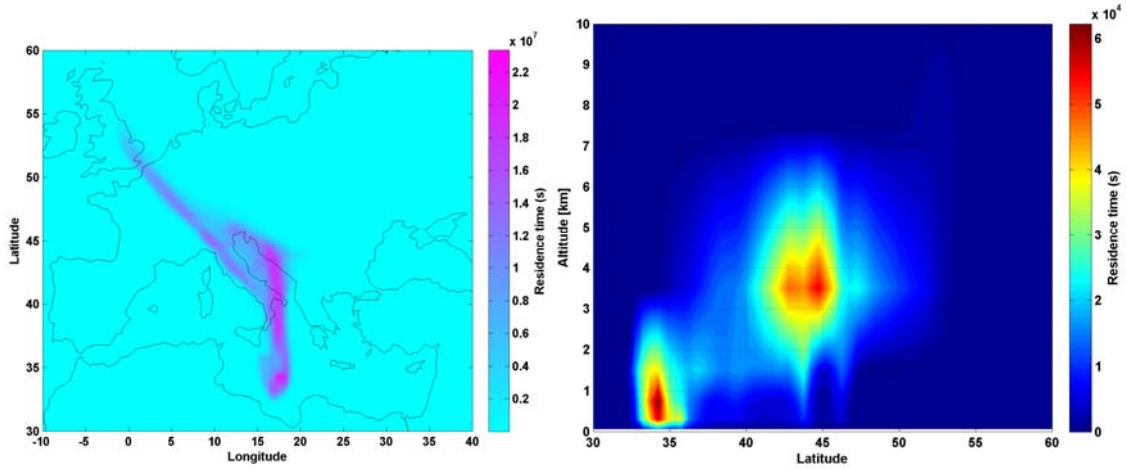

Fig. S4. Residence time distribution (left: latitude vs. longitude, right: latitude vs. altitude) of particles in backward simulations corresponding to (a) maximum and (b) minimum atmospheric PAH concentrations.

References

Alexander, R, Bastrow, T.P., Fisher, S.J., Kagi, R.I., 1995. Geosynthesis of organic compounds - II. Methylation of phenanthrene and alkylphenanthrenes. Geochim. Cosmochim. Acta 59, 4259-4266.

Andreae, M.O., 1991. Biomass burning: its history, use, and distribution and its impact on environmental quality and global climate, in: Global Biomass Burning: Atmospheric, Climatic, and Biospheric Implications (Levine, J.S., ed.), MIT Press, Cambridge, USA, pp. 1–21.

Bi, X., Simoneit, B.R.T., Sheng, G., Fu, J., 2008. Characterization of molecular markers in smoke from residential coal combustion in China. Fuel 87, 112–119.

Calvert, J.G., Atkinson, R., Becker. K.H., Kamens, R.M., Seinfeld, J.H., Wallington, T.J., Yarwood, G., 2002. The mechanisms of atmospheric oxidation of aromatic hydrocarbons, Oxford University Press, New York, 117 pp.

Castro-Jiménez, J., Berrojalbiz, N., Wollgast, J., Dachs, J. , 2012. Polycyclic aromatic hydrocarbons (PAHs) in the Mediterranean Sea: Atmospheric occurrence, deposition and decoupling with settling fluxes in the water column. Environ. Pollut. 166, 40-47.

d'Ortenzio, F., Iudicone, D., de Boyer Montegut, C., Testor, C., Antoine, D., Marullo, S., Santoleri, R., Madec, G., 2005. Seasonal variabilità of the mixed layer depth in the Mediterranean Sea as derived from in situ profiles, Geophys. Res. Lett. 32, L12605.

EU, 1996. Technical guidance document in support of the commissions directive 5 93/67/EEC on risk assessment for the notified substances and the commission regulation (EC) 1488/94 on risk assessment for existing substances.

Franklin, J., Atkinson, R., Howard, P.H., Orlando, J.J., Seigneur, C., Wallington, T.J., Zetzsch, C., 2000. Quantitative determination of persistence in air, in: Evaluation of Persistence and Long-Range Transport of Organic Chemicals in the Environment (Klecka, G.M., et al., eds.), SETAC Press, Pensacola, USA, pp. 7–62.

Jonker, M.T.O., Muijs, B., 2010. Using solid phase micro extraction to determine salting-out (Setschenow) constants for hydrophobic organic chemicals. Chemosphere 80, 223–227.

Kaiser, J.W., Heil, A., Andreae, M.O., Benedetti, A., Chubarova, N., Jones, L., Morcrette, J.J., Razinger, M., Schultz, M.G., Suttie, M., van der Werf, G.R., 2012. Biomass burning emissions estimated with a global fire assimilation system based on observed fire radiative power. Biogeosci. 9, 527-554.

Karickhoff, S.W., 1981. Semiempirical estimation of sorption of hydrophobic pollutants on natural sediments and soils. Chemosphere 10, 833-849.

Lammel, G., Novák, J., Landlová, L., Dvorská, A., Klánová, J., Čupr, P., Kohoutek, J., Reimer, E., Škrdlíková, L., 2010a. Sources and distributions of polycyclic aromatic hydrocarbons and toxicity of polluted atmosphere aerosols, in: Urban Airborne Particulate Matter: Origins, Chemistry, Fate and Health Impacts (Zereini, F., Wiseman, C.L.S., eds.), Springer, Berlin, pp. 39-62

Lammel, G., Klánová, J., Ilić, P., Kohoutek, J., Gasić, B., Kovacić, I., Škrdlíková, L., 2010b. Polycyclic aromatic hydrocarbons on small spatial and temporal scales – II. Mass size distributions and gas-particle partitioning, Atmos. Environ. 44, 5022-5027.

Leppänen, H., Oikari, A., 1999. Occurrence of retene and resin acids in sediments and fish bile from a lake receiving pulp and paper mill effluents. Environ. Toxicol. Chem. 18, 1498–1505.

Pujo-Pay, M., Conan, P., Oriol, L., Cornet-Barthaux, V., Falco, C., Ghiglione, J.-F., Goyet, C., Moutin, T., Prieur, L., 2011. Integrated survey of elemental stoichiometry (C, N, P) from the western to eastern Mediterranean Sea, Biogeosci. 8, 883-899.

Rowe, C.L., Mitchelmore, C.L., Baker, J.E., 2009. Lack of biological effects of water accommodated fractions of chemically-and physically-dispersed oil on molecular, physiological, and behavioral traits of juvenile snapping turtles following embryonic exposure. Sci. Total Environ. 407, 5344-5355.

Schmidl, C., Bauer, H., Dattler, A., Hitzenberger, R., Weissenbroek, G., 2008. Chemical characterisation of particle emissions from burning leaves, Atmos. Environ. 42, 9070–9079.

Schwarzenbach, R.P., Gschwend, P.M., Imboden, D.M., 2003: Environmental Organic Chemistry, 2nd ed., Wiley, Hoboken, USA.

Shen, G., Tao, S., Wei, S., Zhang, Y., Wang, R., Wang, B., Li, W., Shen, H., Huang, Y., Yang, Y., Wang, W., Wang, X., Simonich, S.L., 2012. Retene emission from residential solid fuels in China and evaluation of retene as a unique marker for soft wood combustion. Environ Sci Technol. 46, 4666-4672.

Spivakovsky, C.M., Logan, J.A., Montzka, S.A., Balkanski, Y.J., Foreman-Fowler, M., Jones, D.B.A., Horowitz, L.W., Fusco, A.C., Brenninkmeijer, C.A.M., Prather, M.J., Wofsy, S.C., McElroy, M.B., 2000. Three-dimensional climatological distribution of tropospheric OH: update and evaluation. J. Geophys. Res. 105, 8931–8980.

Stull, R.B., 1988. An introduction to atmospheric boundary layer meteorology, Kluwer, Dordrecht, the Netherlands, 666 pp.

Tsapakis, M., Apsotolaki, M., Eisenreich, S., Stephanou, E.G. , 2006. Atmospheric deposition and marine sedimentation fluxes of polycyclic aromatic hydrocarbons in the Eastern Mediterranean Basin, Environ. Sci. Technol. 40, 4922-4927.

USEPA, 2009. EPI Suite v4.0, Exposure assessment tools and models, US Environmental Protection Agency. http://www.epa.gov/opt/exposure/pubs/episuitedl.

WMO, 2013. Data from Iraklion weather station, World Meteorological Organisation, URL: http://www.ncdc.noaa.gov.